

**Modulating the electronic structure of a hydrogen-bonded organic framework to  
improve the uranium removal by enhancing hydrogen evolution reaction**

Qingsong Zhang <sup>a, \*</sup>, Yuyang Miao <sup>a</sup>, Yang Xiao <sup>b, \*</sup>, Jianwei Hu <sup>a</sup>, Haiyi Gong <sup>a</sup>,  
Qingyi Zeng <sup>a, \*</sup>

<sup>a</sup> School of Resource & Environment and Safety Engineering, University of South  
China, Hengyang 421001, China

<sup>b</sup> School of Nuclear Science and Technology, University of South China, Hengyang  
421001, China

---

\* Corresponding authors.

E-mail addresses: qszhang@usc.edu.cn (QS. Zhang); xiaoyang950529@163.com (Y. Xiao);  
qingyizeng@usc.edu.cn (QY. Zeng)

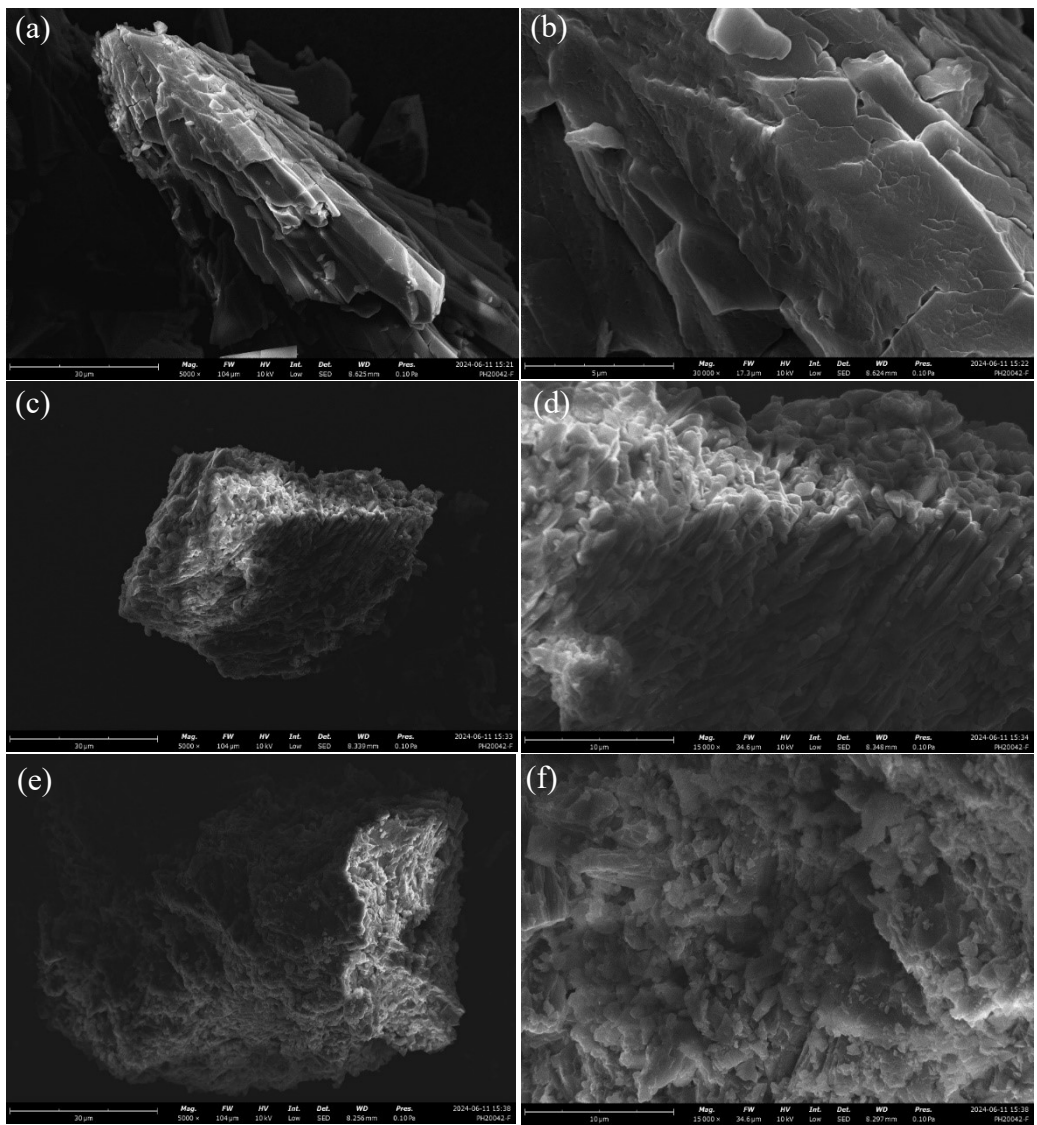


**Fig. S1.** SEM images of (a, b) Co-HOF; (c,d) Co9.5Ni0.5-HOF; (e, f) Co8Ni2-HOF.

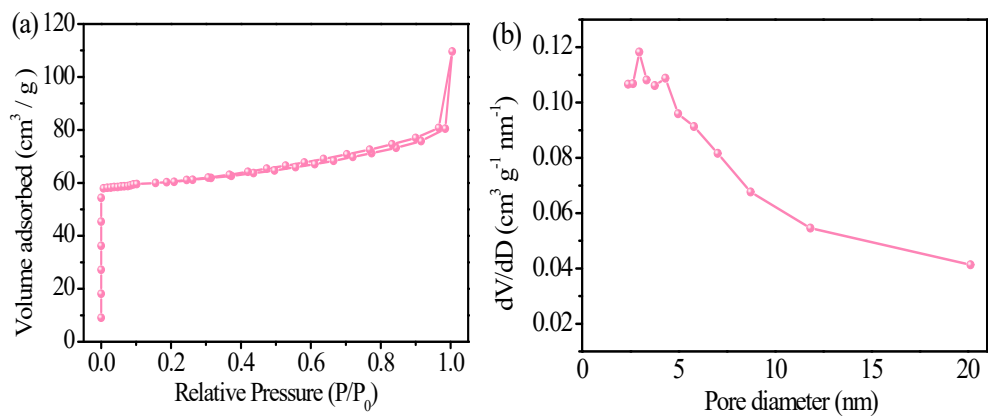


**Fig. S2.** (a) Nitrogen adsorption-desorption isotherms and (b) pore diameter distribution of Co-HOF.

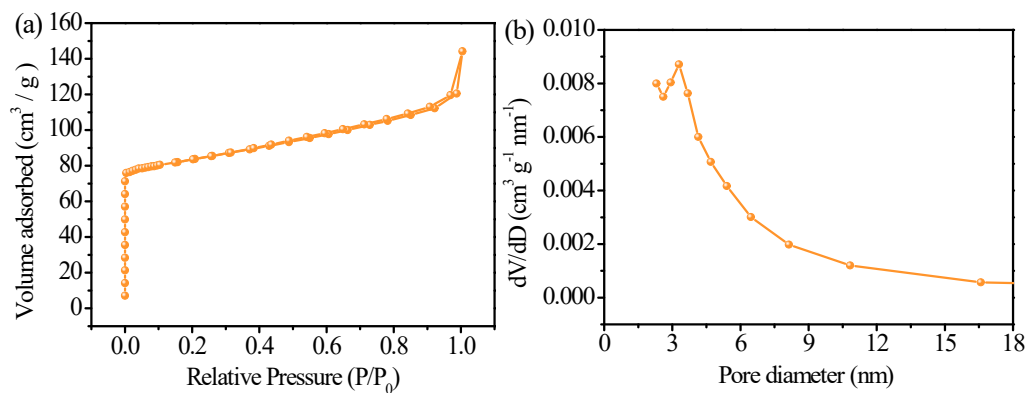


**Fig. S3.** (a) Nitrogen adsorption-desorption isotherms and (b) pore diameter distribution of  $\text{Co}_{9.5}\text{Ni}_{0.5}$ -HOF.

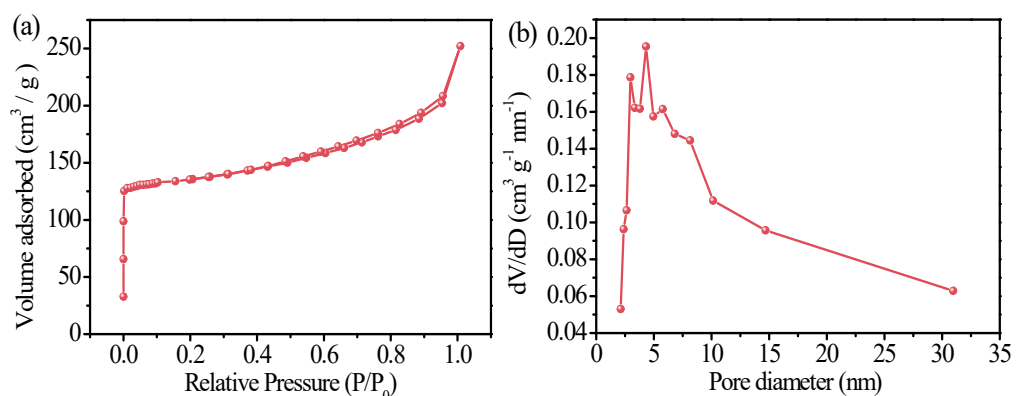


**Fig. S4.** (a) Nitrogen adsorption-desorption isotherms and (b) pore diameter distribution of  $\text{Co}_9\text{Ni}_1$ -HOF.

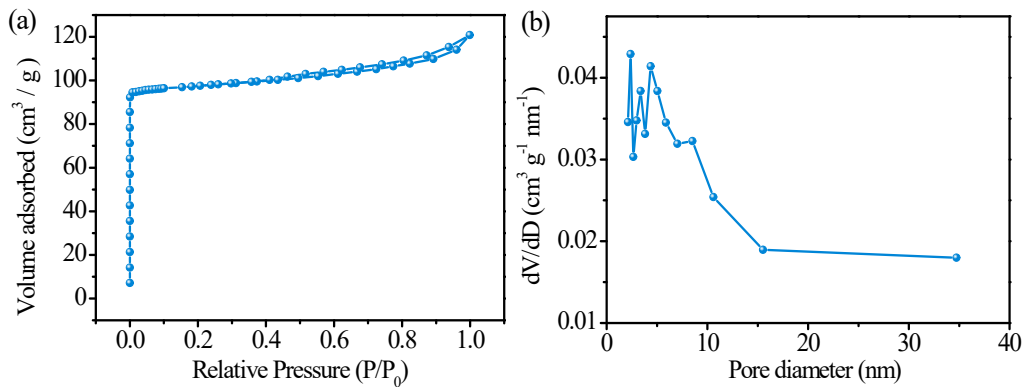


**Fig. S5.** (a) Nitrogen adsorption-desorption isotherms and (b) pore diameter distribution of  $\text{Co}_8\text{Ni}_2$ -HOF.

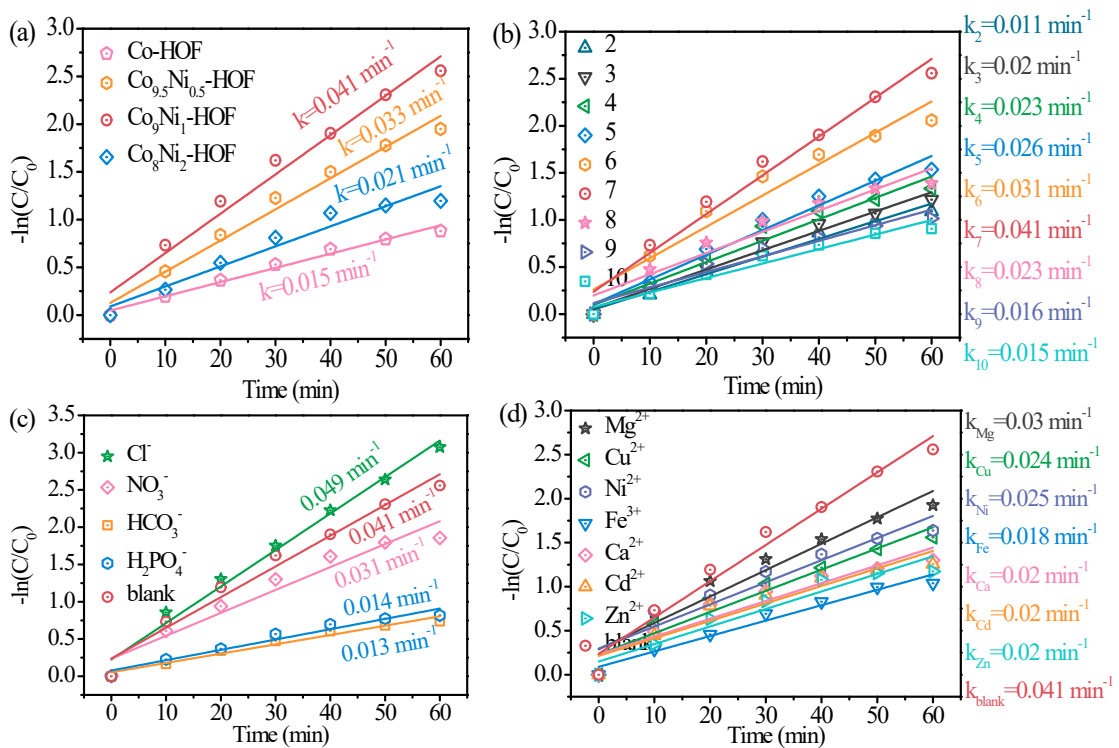


**Fig. S6.** (a) The kinetic rate constant of the  $\text{UO}_2^{2+}$  removal over different photocatalysts; (b-d) The kinetic rate constant of the  $\text{UO}_2^{2+}$  removal for different effects, (b) pH; (c) anions and (d) cations.

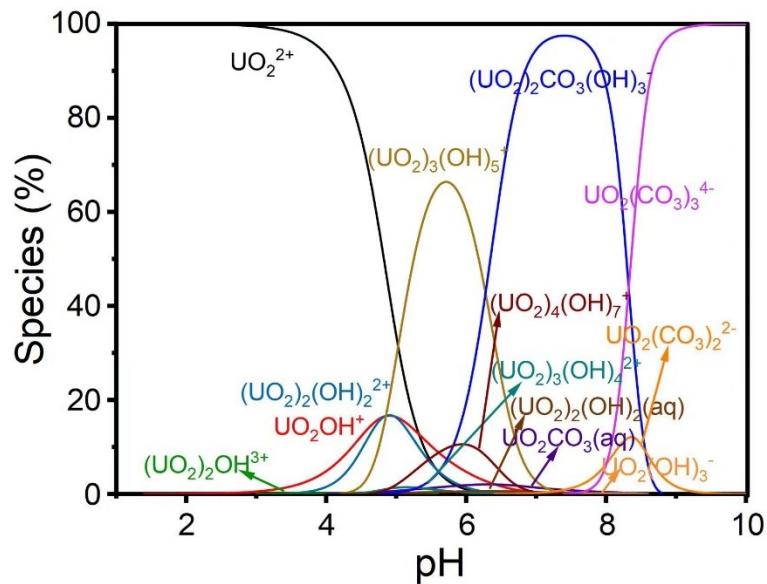


**Fig. S7.** Simulation of U(VI) speciation as a function with different pH.

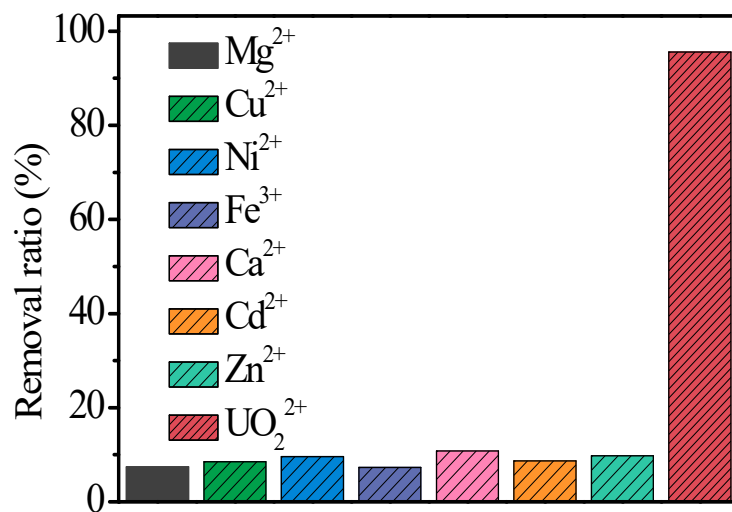


**Fig. S8.** Selective removal of coexistent ions on Co<sub>9</sub>Ni<sub>1</sub>-HOF.

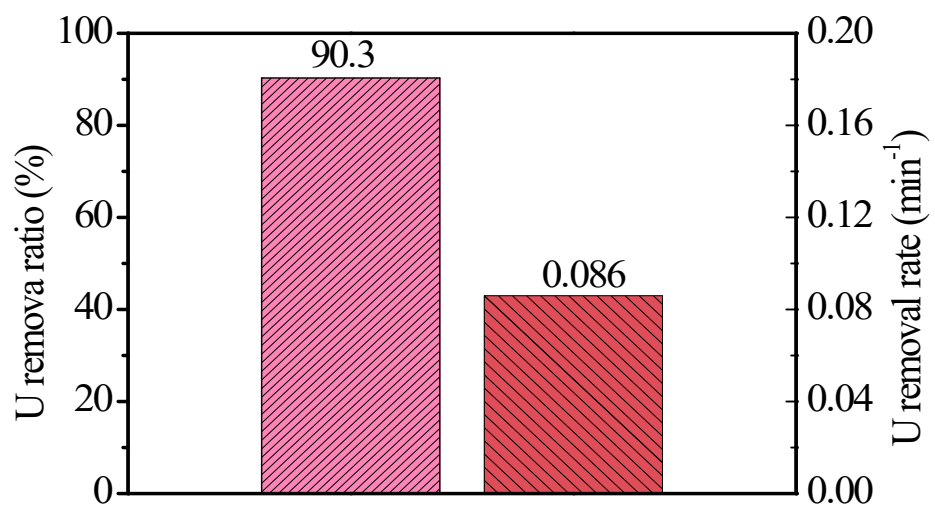


**Fig. S9.** The removal ratio and rate of U in simulated seawater for  $\text{Co}_9\text{Ni}_1$ -HOF photocatalyst

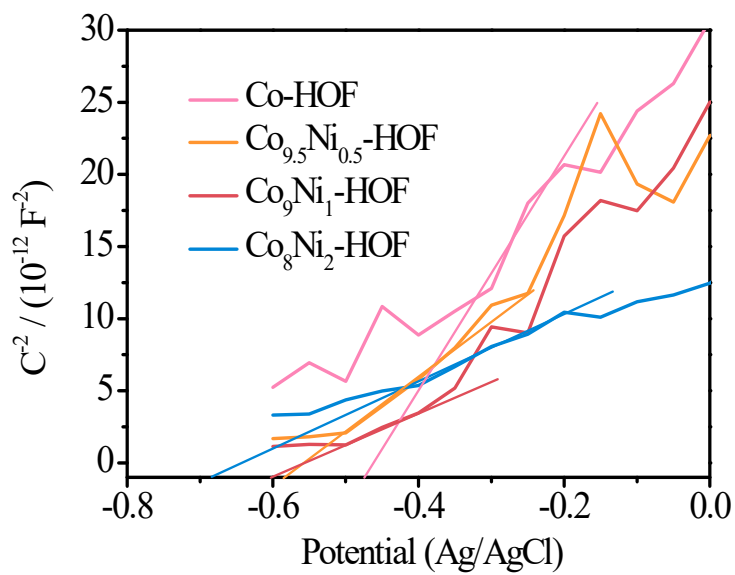


**Fig. S10.** Mott-Schottky plots of the various samples.

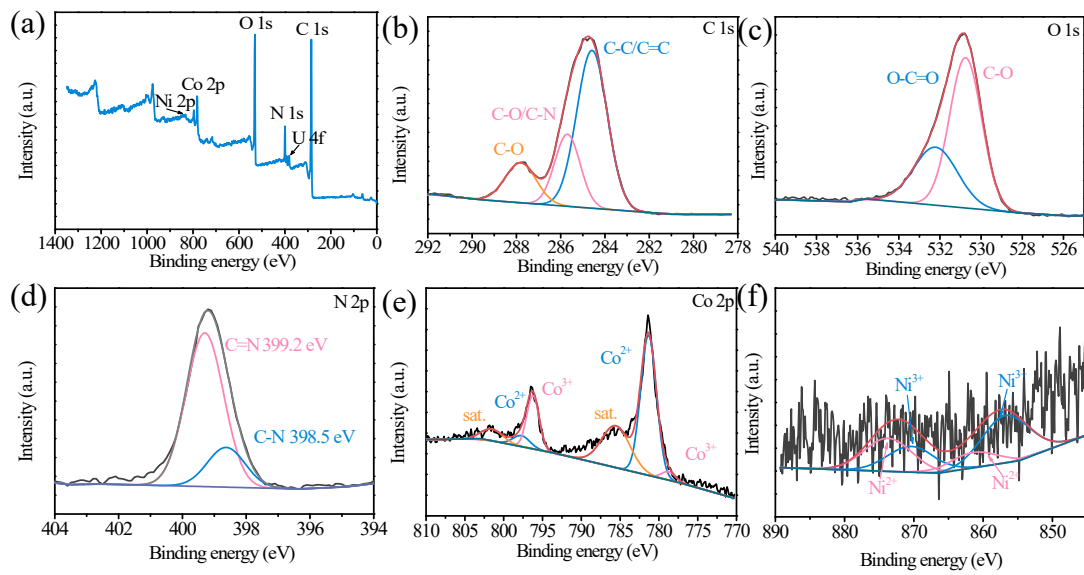


**Fig. S11.** (a) Full XPS region of  $\text{Co}_9\text{Ni}_1\text{-HOF}$ ; high-resolution XPS spectra of (b) C 1s, (c) C 1s, (d) N 2p, (e) Co 2p and (d) Ni 2p after uranium removal.

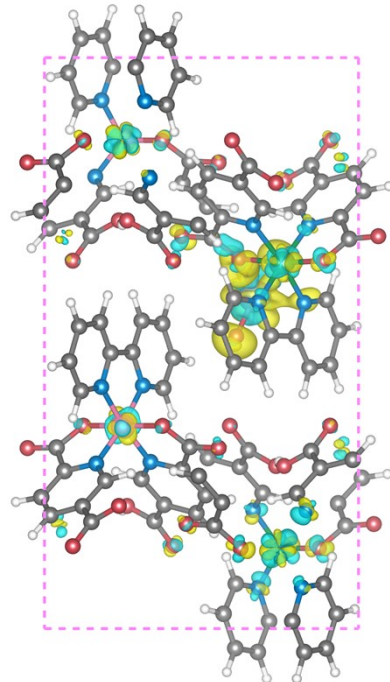


**Fig. S12.** Charge density differences of  $\text{UO}_2^{2+}$  adsorption on  $\text{NiCo-HOF}$ . Yellow indicates electron accumulation, and light blue indicates depletion.

**Table S1.** Surface and pore information of the samples.

Samples	Specific surface area (m <sup>2</sup> /g)	Pore volume (cm <sup>3</sup> /g)	Pore diameter (nm)
Co-HOF	191.62	0.137	2.4
Co <sub>0.5</sub> Ni <sub>0.5</sub> -HOF	308.34	0.192	2.83
Co <sub>9</sub> Ni <sub>1</sub> -HOF	432.66	0.364	3.67
Co <sub>8</sub> Ni <sub>2</sub> -HOF	270.85	0.185	2.86

**Table S2.** The ratio of different valence states over Co<sup>2+</sup>/Co<sup>3+</sup> and Ni<sup>3+</sup>/Ni<sup>2+</sup>

Samples	Co <sup>2+</sup> /Co <sup>3+</sup> (2p <sub>1/2</sub> )	Co <sup>2+</sup> /Co <sup>3+</sup> (2p <sub>3/2</sub> )	Ni <sup>3+</sup> /Ni <sup>2+</sup> (2p <sub>1/2</sub> )	Ni <sup>3+</sup> /Ni <sup>2+</sup> (2p <sub>3/2</sub> )
Co-HOF	1.006	1.018	-	-
Co <sub>9</sub> Ni <sub>1</sub> -HOF	1.008	1.021	1.002	1.003

**Table S3.** Comparison of HER activity with other materials.

Materials	Overpotential (mV)	Reference
Mg <sub>0.99</sub> Ni <sub>0.01</sub> Ga <sub>0.01</sub> Fe <sub>1.99</sub> O <sub>4</sub>	-820	S1
2H-TaS <sub>2</sub>	575	S2
Mo-doped SnS	377	S3
Ni-SAO	837.6	S4
Pd@TiO <sub>2</sub> -H	430	S5
PSS (BiW@PEPS)	361	S6

---

<b>B, P and S-doped Ag<sub>2</sub>WO<sub>4</sub></b>	330	S7
<b>Ni/Ni<sub>3</sub>C/CdS</b>	-1080	S8
<b>Cu-SnO<sub>2</sub>/ZIF-8</b>	364	S9
<b>Cl-doped CuO</b>	400	S10
<b>MoS<sub>2</sub>/BN/rGO</b>	-422	S11
<b>CuO Nanoflowers</b>	1020	S12
<b>Ag@g-C<sub>3</sub>N<sub>4</sub>/r-GO</b>	484	S13
<b>ZnO-Ti<sub>3</sub>C<sub>2</sub></b>	495	S14
<b>MnTiO<sub>3</sub>/g-C<sub>3</sub>N<sub>4</sub></b>	357	S15
<b>Co<sub>0.6</sub>Cu<sub>0.4</sub>Fe<sub>2</sub>O<sub>4</sub></b>	-810	S16
<b>Tetra-carboxylic acid based MOF</b>	391	S17
<b>Co<sub>9</sub>Ni<sub>1</sub>-HOF</b>	355	This work

---

Reference:

- [S1] R. Jasrotia, A. Verma, J. Ahmed, V. Khanna, M. Fazil, S. M. Alshehri, S. Kumari, P. Kumar, T. Ahmad, A. Kandwal, Mg<sub>1-x</sub>Ni<sub>x</sub>Ga<sub>y</sub>Fe<sub>2-y</sub>O<sub>4</sub> nano catalysts for green hydrogen generation with highly efffcient photo/electro catalytic water splitting applications, *Int. J. Hydrogen Energ.*, 2024, **52**, 1228–1240.
- [S2] E. Kovalska, P. K. Roy, N. Antonatos, V. Mazanek, M. Vesely, B. Wu, Zd. Sofer, Photocatalytic activity of twist-angle stacked 2D TaS<sub>2</sub>, npj 2D Mater. Appl. 2021, **68**.
- [S3] S. R. Kadam, S. Ghosh, R. Bar-Ziv, M. Bar-Sadan, Structural transformation of SnS<sub>2</sub> to SnS by Mo doping produces electro/photocatalyst for hydrogen production, *Chem. Eur. J.*, 2020, **26**, 6679-6685.

- [S4] C. L. Wang, H. Yang, J. Du, S. Z. Zhan, Catalytic performance of a square planar nickel complex for electrochemical- and photochemical-driven hydrogen evolution from water, *Inorg. Chem. Commun.* 2021, **131**, 108780.
- [S5] C. Shu, H. Du, W. H. Pu, C. Z. Yang, J. Y. Gong, Trace amounts of palladium-doped hollow TiO<sub>2</sub> nanosphere as highly efficient electrocatalyst for hydrogen evolution reaction, *Int. J. Hydrogen Energ.* 2021, **46**, 1923-1933.
- [S6] R. Manikandan, S. Sekar, S. P. Mani, S. Lee, D. Y. Kim, S. Saravanan, Bismuth tungstate-anchored PEDOT: PSS materials for high performance HER electrocatalyst, *Int. J. Hydrogen Energ.* 2023, **48**, 11746-11753.
- [S7] M. M. Mohamed, M. Khairy, S. Eid, Phosphorous, boron and sulphur-doped silver tungstate-based nanomaterials toward electrochemical methanol oxidation and water splitting energy applications, *Int. J. Hydrogen Energ.* 2024, **50**, 1232–1245.
- [S8] F. Y. Liu, F. Chen, X. Li, A. R. Xu, Z. J. Li, Z. J. Si, Z. Chen, A novel ternary nano-photocatalyst (Ni/Ni<sub>3</sub>C/CdS) for HER and water purification with enhanced photocatalytic activity, *Chem. Eng. J.* 2023, **478**, 147242.
- [S9] D. D. Zhang, H. M. Yang, Y. P. Li, Z. F. Li, N. Gao, W. J. Zhou, Z. H. Liang, High-performance Photoelectrocatalytic Reduction of CO<sub>2</sub> by the hydrophilic-hydrophobic composite Cu-SnO<sub>2</sub>/ZIF-8, *Int. J. Electrochem. Sci.*, 2021, **16**, 150951.
- [S10] D. P. Jaihindh, P. Anand, R. S. Chen, W. Y. Yu, M. S. Wong, Y. P. Fu, Cl-doped CuO for electrochemical hydrogen evolution reaction and tetracycline photocatalytic degradation, *J. Environ. Chem. Eng.* 2023, **11**, 109852.
- [S11] S. Selvaraj, K. Natesan, P. B. Bhargav, A. Nafis, Revolutionizing water

treatment: Exploring the efficacy of MoS<sub>2</sub>/BN/rGO ternary nanocomposite in organic dye treated water for OER and HER applications. *J. Water Process Engineering*, 2023, **54**, 104033.

[S12] F. Naaz, A. Sharma, M. Shahazad, T. Ahmad, Hydrothermally derived hierarchical CuO nanoflowers as an efficient photocatalyst and electrocatalyst for hydrogen evolution, *ChemistrySelect* 2022, **7**, e202201800.

[S13] S. R. Gujula, U. Pal, N. Chanda, S. Karingula, S. Chirra, S. Siliveri, S. Goskula, V. Narayanan, Versatile bifunctional Ag@g-C<sub>3</sub>N<sub>4</sub>/r-GO catalyst for efficient photoand electrocatalytic H<sub>2</sub> production, *Energy Fuels* 2023, **37**, 9722–9735.

[S14] B. Saini, Harikrishna K, D. Laishram, R. Krishnapriya, R. Singhal, R. K. Sharma, Role of ZnO in ZnO nanoflake/Ti<sub>3</sub>C<sub>2</sub> MXene composites in photocatalytic and electrocatalytic hydrogen evolution. *ACS Appl. Nano Mater.* 2022, **5**, 9319–9333.

[S15] F. Li, Y. Zhou, S. T. Xie, Z. L. Wu, Q. J. Wang, Y. N. An, H. H. Huang, Q. Y. He, F. Li, K. Y. Zhao, P. W. Wu, C. L. Yu, In-situ synthesis of 2D Z-scheme MnTiO<sub>3</sub>/g-C<sub>3</sub>N<sub>4</sub> heterostructure for efficient electrocatalytic hydrogen production, *J. Taiwan Inst. Chem. Eng.* 2023, **151**, 105085.

[S16] P. Kotwal, R. Jasrotia, A. V. Nidhi, J. Ahmed, S. Thakur, A. Kandwal, M. Fazil, S. M. Alshehri, T. Ahmad, A. Verma, N. Sharma, R. Kumar, Photo/electrocatalytic green hydrogen production promoted by Ga modified Co<sub>0.6</sub>Cu<sub>0.4</sub>Fe<sub>2</sub>O<sub>4</sub> nano catalysts, *Environ. Res.* 2024, **241**, 117669.

[S17] Q. Qiu, T. Wang, L. H. Jing, K. Huang, D B. Qin, Tetra-carboxylic acid based metal-organic framework as a high-performance bifunctional electrocatalyst for HER

and OER, *Int. J. Hydrogen Energ.* 2020, **45**, 11077-11088.

**Table S4.** *k* values of the different samples.

Samples	Co-HOF	Co <sub>9.5</sub> Ni <sub>0.5</sub> -HOF	Co <sub>9</sub> Ni <sub>1</sub> -HOF	Co <sub>8</sub> Ni <sub>2</sub> -HOF
k values	0.0027	0.0047	0.0068	0.0031